PROCEEDINGS OF THE YEREVAN STATE UNIVERSITY

Chemistry and Biology 2018, **52**(3), p. 147–154

Chemistry

AB INITIO HARTREE–FOCK AND DENSITY FUNCTIONAL THEORY INVESTIGATIONS ON THE POTENTIAL ENERGY SURFACE AND VIBRATIONAL SPECTRA OF DIETHYL SULFONE

Z. Kh. PAPANYAN [*], A. S. MKHITARYAN [**], L. S. GABRIELYAN [***]

Chair of Physical and Colloids Chemistry YSU, Armenia

In this work, *ab initio* Hartree–Fock (RHF/6-311++G(d, p)) and density functional theory (B3PW91/6-311++G(d, p)) investigations on the potential energy surface (PES) and vibrational spectra of diethyl sulfone have been performed. It was found, that diethyl sulfone exists as an equilibrium mixture of four interconverting rotational isomers. The accurate energies of the four minima and the five saddle points located on PES were determined at the above mentioned levels of calculation. The relative populations of the stationary points found have been calculated using Boltzmann distribution law, considering the degeneracy of states. The theoretical IR spectra calculations for all stationary points on the PES have been done as well.

***Keywords*:** diethyl sulfone, potential energy surface, HF, DFT, conformer, IR spectra.

Introduction. Among sulfur-containing compounds sulfones are important and widely used solvents due to their unique physicochemical properties. They also find some niche biomedical and technological applications. It was established that dimethyl sulfone (DMSO2) is always present in small concentrations in human blood and urine [1, 2]. In the recent years, extensive experimental and theoretical investigations were done to study the use of sulfones as components of electrolyte systems in lithium batteries [3–8]. A large literature data set is available on both experimental and computational study of the structure of the first homologue of sulfones, DMSO2 [9–13]. Earlier, the different thermodynamic properties of diethyl sulfone (DESO2), the structural and spectral parameters of lithium chloride/DESO2 systems, as well as the heat of hydration of DESO2 have been calculated by restricted Hartree–Fock and density functional methods [14–16].

Potential energy surface (PES) calculation is important, because it helps us in visualizing and understanding the relationship between potential energy and molecular geometry [17]. PES is the mathematical or graphical relationship between the energy of a molecule and its geometry. The positions of the energy minima on PES correspond to the equilibrium structures of the stable conformers, and the position of the energy maximum along the reaction coordinate connecting these minima defines the transition state. All these points on PES are called statio-

[*] E-mail: z.papanyan@ysu.am; [**] mkhitaryan.ashot@ysu.am; [***] lgabriel@ysu.am

nary points. Mathematically, a stationary point is one, at which the first derivative of the potential energy with respect to each independent coordinate is zero:

$$\partial E/\partial q_1 = \partial E/\partial q_2 = \ldots = \partial E/\partial q_{3N-6} = 0.$$

In smaller systems, which have only a few minima, it is possible to use an accurate approach to describe the entire PES [18]. The quantitative pictures of the large systems with a high degree of freedom need a rigorous mathematical treatment.

The main goal of this study was to extend previous works [15, 16] with new computational results considering identification and characterization of all transition state structures on the potential energy surface (PES), to elucidate all possible allowed interconversion routes between stable structures, activation energy barriers of these transitions and calculations of vibrational spectra of stable conformers as well as mass-averaged IR spectrum of DESO2 in the gas phase. Hartree–Fock (HF) and density functional theory (DFT) methods with expanded basis set [19–21] have been used in the course of this study.

Computational Part. Gaussian 09 computational package [22] was used to perform conformational and vibrational analysis of isolated DESO2 molecule at the both restricted HF and DFT levels of theory. Gaussian B3PW91 hybrid functional was used for DFT, which implements Becke's three-parameter B3 hybrid exchange functional combined with Perdew–Wang's PW91 gradient-corrected correlation functional [23, 24].

First, two-dimensional PES of DESO2 were calculated at RHF/6-311++G(d, p) and B3PW91/6-311++G(d, p) levels of theory by simultaneously changing two dihedral angles, representing spatial orientations of ethyl moieties around C–S bonds in DESO2 molecule. This was accomplished by invoking a relaxed PES scan, where the appropriate dihedral angles were changed in the range of 0–360° in 15° steps, while all other internal coordinates converged to their equilibrium values at each point.

This procedure is not any different from a standard optimization procedure (g09 Opt), except that for a chosen dihedral angle pair the values of the latter are kept "frozen", while remaining 3N-8 variables are let "free" to converge to their values, where the potential energy of the molecule is minimal. Of course the structures obtained this way are not "true" minima, since 2 variables were frozen, but this is needed to construct PES of the molecule in dependence on these variables. Then, to locate "real" minima geometries, apparent near-to-minima structures on the obtained PES were selected (9 structures, further recognized as of 4 different types) and a complete gas phase optimization was performed at the same levels of theory. Similarly, transition state structures were selected near the saddle points on PES and proceeded further (g09 Opt=ts). All stationary points thus obtained (equilibrium geometries of minima as well as transition states) were verified by vibrational frequency calculations. The assignments of the calculated frequencies were done by GaussView 5.0 program, which gives a visual presentation of the vibrational modes.

It is worth to mention, that in Gaussian 09 the default algorithm for both minimizations (optimizations to a local minimum) and optimizations to transition states and higher-order saddle points is the Berny algorithm using GEDIIS in redundant internal coordinates. Convergence criteria were chosen by us to the most stringent (Opt=verytight), with maximum and rms force thresholds equal to $2 \cdot 10^{-6}$ and

$1 \cdot 10^{-6}$ *Hartree*/*Bohr*, the change in energy at the last optimization step is typically below 10^{-13} *Hartree*.

Results and Discussion.

Molecular Structure and Potential Energy Surface. Two structural parameters, the dihedral angles denoted as D1 (C14–C4–S1–C7) and D2 (C10–C7–S1–C4) on Fig. 1, are expected to influence the conformational stability of DESO2 molecule the most. These represent two ethyl group rotations around C–S bonds, where each one, if considered separately, normally should lead to 3 staggered and 3 eclipsed conformations. Since both dihedral angles are changed independently during the free internal rotations in molecule, 36 (6^2) mutual combinations are possible in total. Among them 9 (3^2) are expected to be of minima, 9 (3^2) of maxima and 18 ($2 \cdot 3^2$) of transition states.

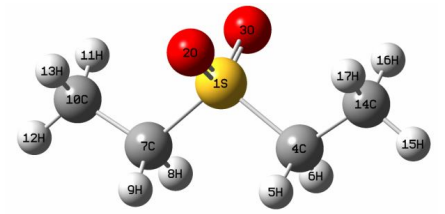

Fig. 1. Optimized global minimum structure of diethyl sulfone molecule.

To locate and identify all the above mentioned stationary points, relaxed PES scans of DESO2 in gas phase at RHF/6-311++G(d, p) and B3PW91/6-311++G(d, p) levels of theory were performed and three-dimensional PES were obtained, as shown in Fig. 2 a, b. From the examination of PES surfaces obtained by both methods 9 minima points, which are attributed to the different conformational isomers of DESO2, can be clearly identified. However, due to the fact that both substituents attached to SO_2 group are identical, degenerate states with the same structures and energies are present on PES, and only 4 of the 9 minima are found to be unique. The same issue arising from the symmetry leads to the degeneracy of transition states, thus of the total 18 states observed on PES only 5 are non-identical. The nature of all stationary points on the PES was verified by complete gas phase optimization and vibrational analysis at the same level of theory.

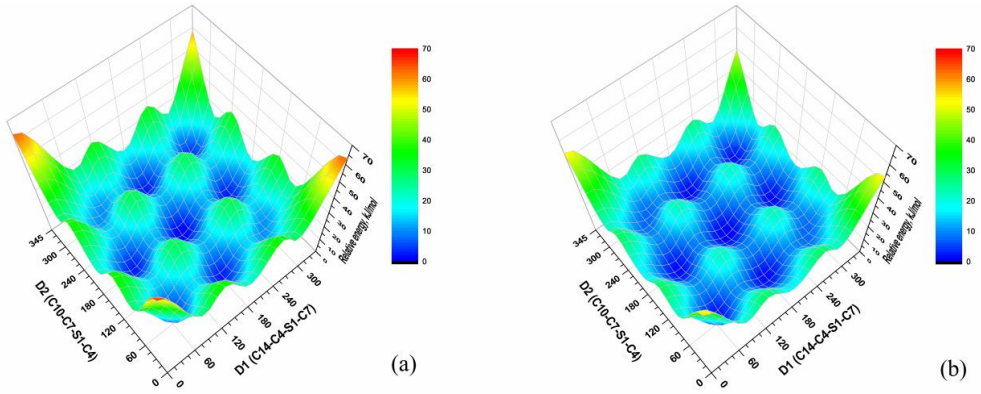

Fig. 2. Potential energy surface of diethyl sulfone according to the RHF/6-311++G(d, p) (a) and B3PW91/6-311++G(d, p) (b) calculations.

Thus, DESO2 exists as an equilibrium mixture of four rotational conformers: one global minimum structure (II) with dihedral angles D1and D2 equal to 180°, fourfold degenerate structure (III) with D1=67° and D2=177° (and DI/D2 –67°/177°, 177°/67°, 177°/–67°), doubly degenerate structures (I) with D1=64° and D2=64° (–64/–64) and (IV) with D1=71° and D2=–84° (–84/–71) (RHF/6-311++G(d, p)). These conformers are converted into each other through five transition states: (I↔III), (II↔III), (III↔IV) and (I↔VI) transitions are fourfold degenerate, and (III↔III) transition is doubly degenerate. In contrast to stable conformers, vibrational analysis of all transition state structures reveals one imaginary frequency, which serves us to confirm their nature. It is worth to note here, that not for each of the conformers it is possible to directly convert to other structure, i.e. there's not always single transition state existing to connect two arbitrary chosen ground states.

Therefore, some conformational interconversions take place through more than one transition states and more than two ground states are involved. These "forbidden" direct conversions for DESO2 molecule are identified as I↔II, II↔IV particularly. On the other hand, one transition state was identified, connecting the same ground states at the "both ends", particularly for the III↔III conversion. The optimized structures of all conformers and transition states, optimized at RHF/6-311++G(d, p) are presented in Fig. 3, and the energy diagrams, connecting all possible "allowed" transitions are in Fig. 4.

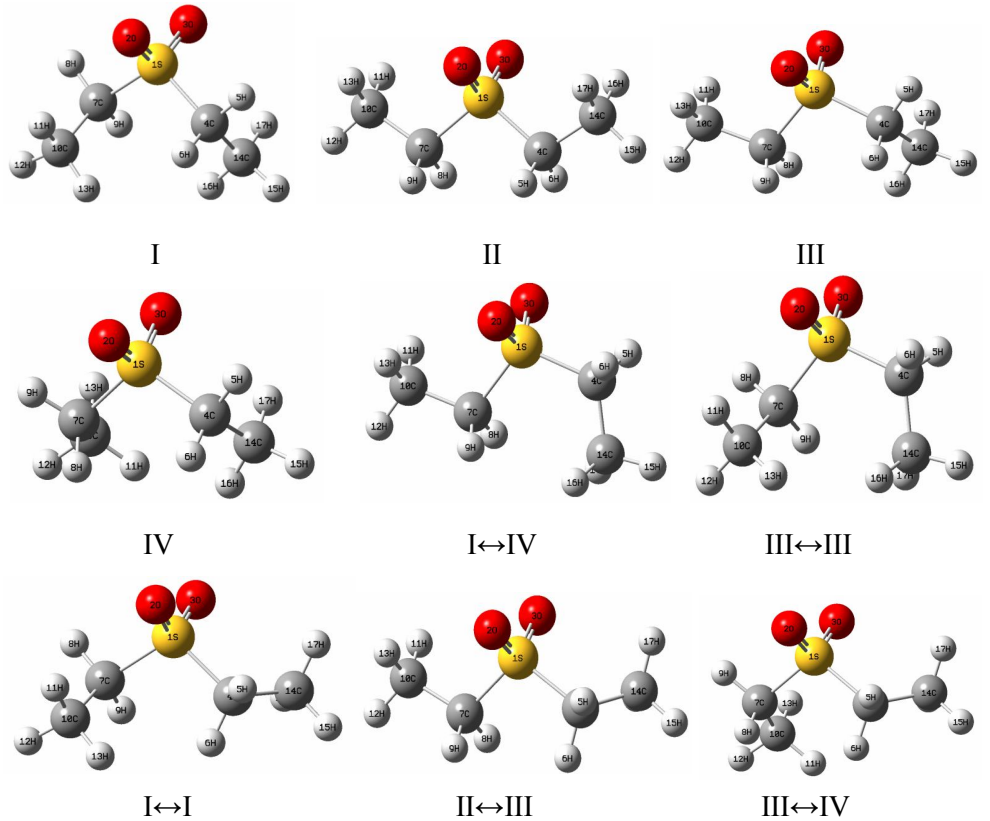

Fig. 3. Optimized geometric structures for the 4 conformers and the 5 conformational transition states of diethyl sulfone molecule, optimized at the RHF/6-311++G(d, p) level of theory.

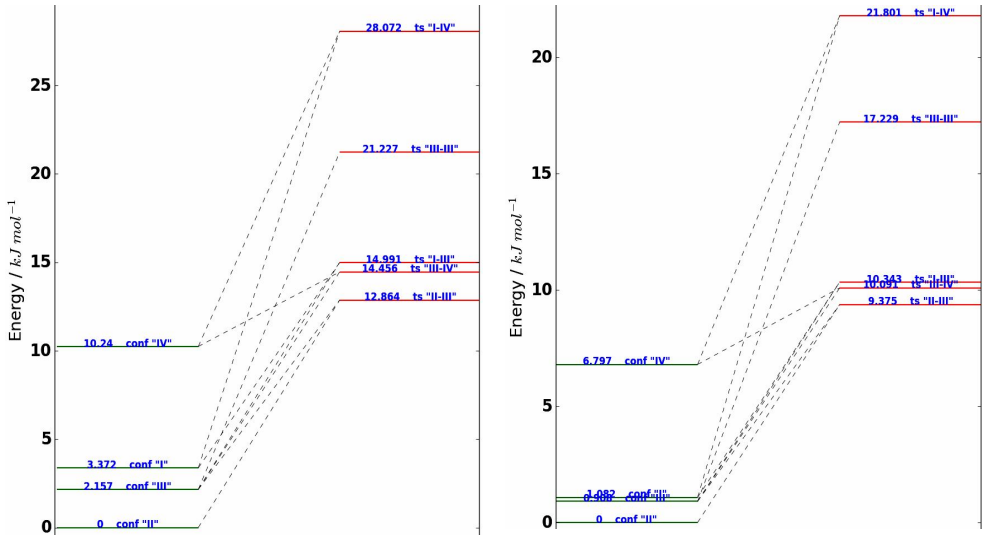

Fig. 4. Potential energy diagrams for diethyl sulfone molecule. All stationary points with the links showing "allowed" interconversion routes at the RHF/6-311++G(d,p) and B3PW91/6-311++G(d,p) levels of theory.

The relative populations of equilibrium conformations (P_i) of DESO2 have been calculated from the Boltzmann distribution taking into account the degree of degeneracy

$$P_i = \frac{g_i e^{-\varepsilon_i / k_B T}}{\sum_i g_i e^{-\varepsilon_i / k_B T}}, \quad (1)$$

where ε_i is the potential energy of i-th conformers; g_i is the degree of degeneracy; k_B is the Boltzmann constant; T is the absolute temperature.

P_i of DESO2 at 298 K calculated by using the Eq. (1) as well as absolute and relative energies of stable conformers and transitions states are given in Table.

According to the calculations, the most energetically favorable conformer is conformer II, which has the smallest dipole moment, and, reciprocally, the conformers with higher energy have stronger dipole moments. Taking into account the degeneracy of the conformers, the percentage of conformer II in the gas phase at 298 K is only 31.1% (RHF) or 19.2% (B3PW91), which indicates that this conformer could not be considered as predominant specie, despite of it being the lowest energy state. The predominant structure of DESO2 molecule in the gas phase with 52–53% was found to be the conformer III. It should be noted that taking into account the zero-point energy (which are in the range 0.151602–0.151724 *Hartree* (RHF) and 0.141902–0.142042 *Hartree* (B3PW91)) does not affect significantly the values of P_i, for example the percentage of conformer II is 31.2% (RHF) and of conformer III is 52.3% (RHF).

Among five transition states, II↔III transition has the lowest energy (see Table). The energy of four other transition states are considerably higher, the energy increases in the series II↔III<III↔IV<I↔III<III↔III<I↔IV regardless of calculation methods. On the other hand, the value of activation barriers (in the forward direction) increases in the series I↔III<III↔IV<II↔III<III↔III<I↔IV in the case

of RHF/6-311++G(d, p), and in the series III↔IV<I↔III<II↔III<III↔III<I↔IV in the case of B3PW91/6-311++G(d, p) calculations. The lowest barrier was predicted for the III↔IV reverse direction, which shows the flat region of the surface. Barriers span a wide range from 3.3 to 24.7 *kJ/mol*.

Characteristics and selected calculation data (degeneracy, g, energy, E, relative energy, ΔE, relative population, P_i, dipole moment, μ, imaginary frequency, ν_{im}, stretching vibrations of SO_2 group) of conformers of diethyl sulfone and the corresponding transition states calculated at the RHF/6-311++G(d, p) and B3PW91/6-311++G(d, p) levels of theory

RHF/6-311++G(d, p)							
Conformer	*g*	*E*, *Hartee*	Δ*E*, *kJ/mol*	P_i	μ, *D*	ν(SO)as, cm^{-1}	ν(SO)s, cm^{-1}
I	2	–704.568289106	3.372	0.159	5.63	1396.53	1218.60
II	1	–704.569573547	0.000	0.311	5.13	1423.87	1225.45
III	4	–704.568751822	2.157	0.520	5.37	1410.94	1223.43
IV	2	–704.565673507	10.240	0.010	5.54	1402.47	1223.15
Transition state	*g*	*E*, *Hartee*	Δ*E*, *kJ/mol*	E_a (forward), *kJ/mol*	E_a (reverse), *kJ/mol*	μ, *D*	ν_{im}, cm^{-1}
I↔III	4	–704.563863681	14.991	11.619	12.834	5.47	–98.09
II↔III	4	–704.564673772	12.864	12.864	10.707	5.25	–92.72
III↔IV	4	–704.564067518	14.456	12.299	4.216	5.50	–82.09
I↔IV	4	–704.558881628	28.072	24.700	17.832	5.77	–125.75
III↔III	2	–704.561488734	21.227	19.070	19.070	5.61	–117.79
B3PW91/6-311++G(d, p)							
Conformer	*g*	*E*, *Hartee*	Δ*E*, *kJ/mol*	P_i	μ, *D*	ν(SO)as, cm^{-1}	ν(SO)s, cm^{-1}
I	2	–706.987441295	1.082	0.249	5.12	1275.68	1117.05
II	1	–706.987853562	0.000	0.192	4.65	1311.91	1122.40
III	4	–706.987507635	0.908	0.534	4.88	1291.30	1120.50
IV	2	–706.985264698	6.797	0.025	5.02	1287.83	1139.34
Transition state	*g*	*E*, *Hartee*	Δ*E*, *kJ/mol*	E_a (forward), *kJ/mol*	E_a (reverse), *kJ/mol*	μ, *D*	ν_{im}, cm^{-1}
I↔III	4	–706.983913998	10.343	9.261	9.435	4.96	–87.65
II↔III	4	–706.984282693	9.375	9.375	8.467	4.75	–82.79
III↔IV	4	–706.984010268	10.091	9.183	3.294	5.00	–76.03
I↔IV	4	–706.979550010	21.801	20.719	15.004	5.26	–112.18
III↔III	2	–706.981291217	17.229	16.321	16.321	5.11	–106.11

IR Spectrum of DESO2. In order to verify the character of all stationary points on the potential energy surface fundamental harmonic vibration frequency calculations for all conformers have been performed at RHF/6-311++G(d, p) and B3PW91/6-311++G(d, p) levels of theory. Earlier, these methods showed good agreement between experimental and theoretical IR spectra of DMSO2 [15]. The calculated IR spectra of four stable conformers of DESO2 and their mass-weighted spectra (taking into account their relative populations) are presented in Fig. 5. DESO2 molecule has 45 fundamental vibration modes, which are all IR active.

The intensity and position of different modes are found to be very sensitive to the conformation state of the DESO2 molecule. In general sulfones are characterized by two strong absorptions between 1400–1000 cm^{-1}, which are attributed to

the antisymmetric and symmetric stretching vibrations of the SO_2 group. As can be seen from enlarged graph, the greatest difference between the conformer's spectra is observed for the antisymmetric stretching vibrations of the SO_2 group, whereas the symmetric stretching vibrations of the SO_2 group do not strongly depend on the rotation of ethyl groups. As was already mentioned, in contrast to stable conformers, vibrational analysis of all transition state structures reveals one imaginary frequency, which are listed in Table.

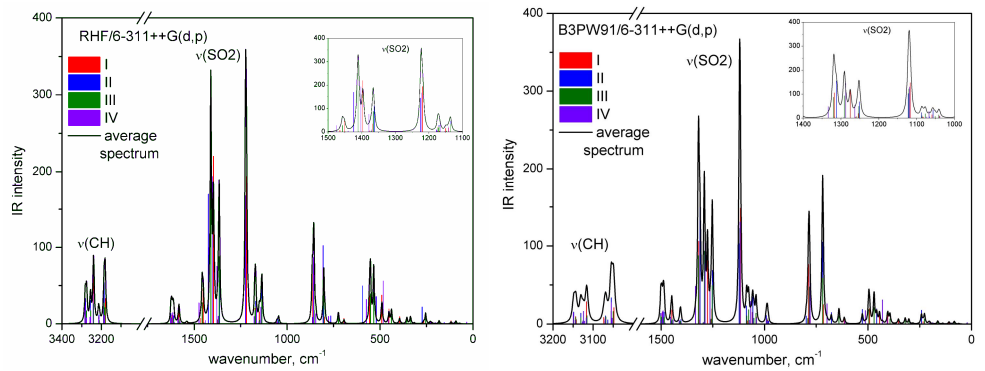

Fig. 5. IR spectra of four stable conformers of DESO2 and their mass-weighted spectra calculated at the RHF/6-311++G(d, p) and B3PW91/6-311++G(d, p) levels of theory.

Conclusion. Thus, it was found that besides 4 stable conformers of DESO2, 5 transition state structures are located on PES. Their geometries, energies and degeneracies were determined, allowed interconversion routes between stable structures were identified. It is shown, that direct conversion of some structures to the others is not always allowed, while for one structure the conversion leads to its original geometry. Activation barrier energies are in the 3.3 to 24.7 *kJ/mol* range.

From the comparison of the vibrational spectra of the stable conformers it was found that the antisymmetric stretching vibrations of the SO_2 group are very sensitive to the conformation of DESO2 molecule, leading to the broadening of that peak in the mass averaged spectrum.

We thank Dr. Y. Mamasakhlisov and the Faculty of Physics for providing access to the Gaussian 09 software package and the computer cluster.

This work was partially supported by the RA MES SCS, in the frame of the research project N 18T-1D086.

Received 21.06.2018

REFERENCES

1. **Rose E.S**. Detection of Dimethyl Sulfone in the Human Brain by *in vivo* Proton Magnetic Resonance Spectroscopy. // Magn. Reson. Imaging, 2000, v. 18, p. 95–98.
2. **Engelke U.F.H., Tangerman A., Willemsen M.A.A.P., Moskau D., Loss S., Mudd S.H., Wevers R.A.** Dimethyl Sulfone in Human Cerebrospinal Fluid and Blood Plasma Confirmed by One-dimensional $^{1}H^{-13}C$ NMR. // NMR Biomed., 2005, p. 331–336.

3. **Linden D., Reddy T.B.** Handbook of Batteries. McGraw-Hill, 2001, 1457 p.
4. **Xu K., Angell C.A.** Sulfone-Based Electrolytes for Lithium-Ion Batteries. // J. Electrochem. Soc., 2002, v. 149, p. A920–A926.
5. **Tarascon J.-M., Armand M.** Issues and Challenges Facing Rechargeable Lithium Batteries. // Nature, 2001, v. 414, p. 359–367.
6. **Sun X.-G., Angell C.A.** New Sulfone Electrolytes. Part II: Cyclo Alkyl Group Containing Sulfones. // Solid State Ionics, 2004, v. 175, p. 257–260.
7. **Abouimrane A., Belharouak I., Amine K.** Sulfone-Based Electrolytes for High-Voltage Li-Ion Batteries. // Electrochem. Commun., 2009, v. 11, p. 1073–1076.
8. **Wang Y., Xing L., Li W., Bedrov D.** Why Do Sulfone-Based Electrolytes Show Stability at High Voltages? Insight from Density Functional Theory. // J. Phys. Chem. Lett., 2013, v. 4, p. 3992−3999.
9. **Clark T., Murray J. S., Lane P., Politzer P.** Why Are Dimethyl Sulfoxide and Dimethyl Sulfone Such Good Solvents? // J. Mol. Model., 2008, v. 14, p. 689–697.
10. **Givan A., Grothe H., Loewenschuss A. and Nielsen C.,** Infrared Spectra and *ab initio* Calculations of Matrix Isolated Dimethyl Sulfone and Its Water Complex. // Phys. Chem. Chem. Phys., 2002, v. 4, p. 255–263.
11. **Allinger N.L., Fan Y.,** Molecular Mechanics Calculations (MM3) on Sulfones. // J. Comp. Chem., 1993, v. 14, p. 655–666.
12. **Clever H.L., Westrum E.F.** Dimethyl Sulfoxide and Dimethyl Sulfone. Heat Capacities, Enthalpies of Fusion, and Thermodynamic Properties. // J. Phys. Chem., 1970, v. 74, p. 1309–1317.
13. **Gabrielyan L.S., Markarian S.A., Weingärtner H.** Dielectric Spectroscopy of Dimethyl Sulfone Solutions in Water and Dimethylsulfoxide. // J. Mol. Liq., 2014, v. 194, p. 37–40.
14. **Mkhitaryan A.S., Papanyan Z.K., Gabrielyan L.S.** Quantum Chemical Study on the Solvation of Lithium Chloride in Dimethyl- and Diethylsulfones. // Proceedings of the YSU. Chemistry and Biology Sciences, 2018, v. 52, № 1, p. 10–19.
15. **Mkhitaryan A.S., Papanyan Z.K., Gabrielyan L.S., Markarian S.A.** Theoretical *ab initio* Calculation of Entropy and Heat Capacity of Dialkylsulfones in the Gas Phase. // Chem. J. Arm., 2018, v. 71, № 1, p. 13–22.
16. **Mkhitaryan A.S., Papanyan Z.K., Gabrielyan L.S., Markarian S.A.** Heat of Hydration of Diethylsulfone by Quantum Chemical Calculation. // Izv. Vyssh. Uchebn. Zaved. Khim., Khim. Tekhnol., 2018, v. 61, № 8, p. 17–21.
17. **Lewars E.G.** Computational Chemistry (2nd ed.). Springer Science+Business Media, 2011, 664 p.
18. **Becker O.M.** Principial Coordinate Maps of Molecular Potential Energy Surfaces. // J. Comp. Chem., 1998, v. 19, № 11, p. 1255–1267.
19. **Jensen F.** Introduction to Computational Chemistry. John Wiley & Sons Ltd, 2006, 600 p.
20. **Hohenberg P., Kohn W.** Inhomogeneous Electron Gas. // Physical Review, 1964, v. 136, p. B864–B871.
21. **Kohn W., Sham L.J.** Self-Consistent Equations Electron Gas. // Physical Review, 1965, v. 140, p. A1133–A1138
22. Gaussian 09, Revision D.01, **Frisch M.J., Trucks G.W., Schlegel H.B., Scuseria G.E., Robb M.A., Cheeseman J.R., Scalmani G., Barone V., Mennucci B., Petersson G.A., Nakatsuji H., Caricato M., Li X., Hratchian H.P., Izmaylov A.F., Bloino J., Zheng G., Sonnenberg J.L., Hada M., Ehara M., Toyota K., Fukuda R., Hasegawa J., Ishida M., Nakajima T., Honda Y., Kitao O., Nakai H., Vreven T., Montgomery J.A., Jr., Peralta J.E., Ogliaro F., Bearpark M., Heyd J.J., Brothers E., Kudin K.N., Staroverov V.N., Keith T., Kobayashi R., Normand J., Raghavachari K., Rendell A., Burant J.C., Iyengar S.S., Tomasi J., Cossi M., Rega N., Millam J.M., Klene M., Knox J.E., Cross J.B., Bakken V., Adamo C., Jaramillo J., Gomperts R., Stratmann R.E., Yazyev O., Austin A.J., Cammi R., Pomelli C., Ochterski J.W., Martin R.L., Morokuma K., Zakrzewski V.G., Voth G.A., Salvador P., Dannenberg J.J., Dapprich S., Daniels A.D., Farkas O., Foresman J.B., Ortiz J.V., Cioslowski J., Fox D.J.** Gaussian Inc., Wallingford CT, 2013.
23. **Becke A.D.** Density-Functional Exchange-Energy Approximation with Correct Asymptotic-Behavior. // Phys. Rev. A, 1988, v. 38, p. 3098–3100.
24. **Burke K., Perdew J.P., Wang Y.** In Book: Electronic Density Functional Theory "Recent Progress and New Directions" (eds. J.F. Dobson, G. Vignale, M.P. Das). Plenum, 1998.